https://doi.org/10.5194/cp-2021-20
Preprint. Discussion started: 15 March 2021

Climate of the Past Discussions
Open Access

The 4.2 ka event in East Asian monsoon region, precisely reconstructed by multi-proxies of stalagmite

Chao-Jun Chen [a, b, c★], Dao-Xian Yuan [b, d], Jun-Yun Li [b *], Xian-Feng Wang [c], Hai Cheng [e], You-Feng Ning [e], R. Lawrence Edwards [f], Yao Wu [b], Si-Ya Xiao [b], Yu-Zhen Xu [b], Yang-Yang Huang [b], Hai-Ying Qiu [b], Jian Zhang [g], Ming-Qiang Liang [h], Ting-Yong Li [a ★ *]

[a] *Yunnan Key Laboratory of Plateau Geographical Processes & Environmental Changes, Faculty of Geography, Yunnan Normal University, Kunming 650500, China*

[b] *Chongqing Key Laboratory of Karst Environment, School of Geographical Sciences; Southwest University, Chongqing 400715, China*

[c] *Asian School of the Environment, Nanyang Technological University, Singapore*

[d] *Karst Dynamic Laboratory, Ministry of Land and Resources, Guilin 541004, China*

[e] *Institute of Global Environmental Change, Xi'an Jiaotong University, Xi'an 710049, China*

[f] *Department of Earth Sciences, University of Minnesota, Minneapolis, MN, USA.*

[g] *Environnements et Paléoenvironnements Océaniques et Continentaux (EPOC), UMR CNRS, 5805, Université de Bordeaux, 33615 Pessac Cedex, France*

[h] *Department of Geosciences, National Taiwan University, Taipei 106, Taiwan, China*

★ These authors contributed equally to this work

* Corresponding authors: Ting-Yong Li and Jun-Yun Li

E-mail: jxljy@swu.edu.cn; cdlity@163.com

https://doi.org/10.5194/cp-2021-20
Preprint. Discussion started: 15 March 2021

Climate of the Past Discussions

Abstract

The 4.2 ka event is one of the most salient features of global climate change in the mid-late Holocene and influenced on the evolution of ancient civilizations. Although a lot of paleoclimate reconstructions have focused on it, the detailed structure and driving mechanism of the 4.2 ka event is still unclear. In this study, the variation of Asian summer monsoon (ASM) during 5000–3000 yr BP was reconstructed by using high-precision U-Th dating (average resolution of 7 yr) and multi-proxies ($\delta^{13}C$, $\delta^{18}O$, Ba/Ca, Sr/Ca, Mg/Ca) of stalagmite YK1306 from Yangkou Cave in southwestern China. The results showed that that the ASM weakened and precipitation decreased during 4600–4330 yr BP and 4070–3700 yr BP. During 4330–4070 yr BP, the ASM became strong, and precipitation increased. The multi-proxies variation of YK1306 showed a "weak-strong-weak" structure of the ASM during the 4.2 ka event, which reappeared in different geologic records. However, westerlies and Australian-Indian summer monsoon (AISM) both showed the opposite change pattern (strong-weak-strong) with the ASM. This was resulted by the different phases of North Atlantic Oscillation (NAO) on a centennial scale, which regulated by the Atlantic Meridional Overturning Circulation (AMOC). In positive NAO-like, the strength of Azores high and westerly wind restrained the intensity of ASM. Thus, the ASM and the Middle East regions experienced bimodal drought and increased dust flux from the north in both regions during the 4.2 ka event. The strengthened meridional winds in the westerlies-dominated climatic regime (WDCR) lead more water vapor from the Indian Ocean and Arabian Sea transporting to in the WDCR, and subsequently increases precipitation in the

https://doi.org/10.5194/cp-2021-20
Preprint. Discussion started: 15 March 2021

WDCR. Meanwhile, the weakening of the AMOC results in the southward migration of the Intertropical Convergence Zone (ITCZ) and strengthens the AISM in the southern Hemisphere, finally results in the opposite change of the AISM contrast to the ASM. In addition, the strong ASM in the era of the Chinese Xia Dynasty maybe produce frequent ancient floods, which led to the decline of Longshan and Liangzhu cultures. The weakening of the ASM after 4070 yr BP contributed to the successful regulation of the ancient floodwaters by Dayu in Chinese history. Therefore, it is maybe credible that the official age for the establishment of the Xia Dynasty in 4070 yr BP. Benefit from the comprehensive comparison and analysis based on the unprecedented high-precise chronology, high-resolution and multi-proxy's stalagmite records, this study not only detailed described the evolution of the ASM during the 4.2 ka event, but also is conducive to verify the age of the first dynasty of China (the Xia Dynasty), and the legend of Dayu.

1. Introduction

Different geological carriers (Ice cores, stalagmites, loess, lake sediments, marine sediments, etc.) in the world have indicated that the 8.2 ka and 4.2 ka events affected global climate change in Holocene (Alley et al., 1997; Kobashi et al., 2007; Cheng et al., 2009; Berkelhammer et al., 2012; Kathayat et al., 2018; Railsback et al., 2018). The International Commission on Stratigraphy (ICS) added two Golden Spikes to the latest international stratigraphic chronology updated in July 2018. Based on 8.2 ka and 4.2 ka, the Holocene was divided into three periods: Greenlandian, Northgrippian and

https://doi.org/10.5194/cp-2021-20
Preprint. Discussion started: 15 March 2021

Climate of the Past Discussions

Meghalayan. The previous studies have suggested that the sudden dam break of Lakes Agassiz and Ojibway lake (AOL) at 8470 ± 300 yr BP triggered the 8.2 ka event (Alley et al., 1997; Barber et al., 1999; Kobashi et al., 2007; Cheng et al., 2009; Daley et al., 2011). The ASM showed a double weak structure during the 8.2 ka event (Cheng et al., 2009; Tan et al., 2020). But what drove this double weak structure is still unclear. Compared with 8.2 ka event, the structure, duration and driving mechanism of 4.2 ka event are more ambiguous (Zhang et al., 2018; Tan et al., 2020). Although the 4.2 ka event is very significant in the global geological records, the study on the 4.2 ka event is still insufficient in the East Asian monsoon region (Zhang et al., 2018; Xiao et al., 2018; Tan et al., 2020). The 4.2 ka event reconstructed from many geological records indicated that it was only a cold and dry climate event (Berkelhammer et al., 2012; Wu et al., 2016; Weiss, 2016; Xiao et al., 2018; Ran et al., 2019; Xiao et al., 2019). However, recent simulations showed that the 4.2 ka event was also double weak structure (Yan and Liu, 2019; Ning et al., 2019). Carolin et al. (2019) suggested that the 4.2 ka event may be larger in magnitude and longer in duration than previous study. A large number of studies have shown that the 4.2 ka event caused the fall of Mesopotamian civilization, Indian civilization, Egyptian civilization and Chinese civilization (Shi et al., 1992; Stanley et al., 2003; Sletten et al., 2013; Kathayat et al., 2018; Railsback et al., 2018; Xiao et al., 2018). According to numerous historical data of China, it was speculated that there were floods disaster around 4200 yr BP (Wu et al., 2005; Huang et al., 2011; Wu et al., 2016). It may lead to the fall of Longshan Culture in northern China and Liangzhu Culture in the lower reaches of the Yangtze River (Shi et al., 1992; Dong et

https://doi.org/10.5194/cp-2021-20
Preprint. Discussion started: 15 March 2021

Climate of the Past
Discussions

al., 2018). The research on the exact time and cause of the floods can provide evidence for the ancient Chinese civilization and the origin of the first dynasty, Xia Dynasty (Wu et al., 2005; Wu et al., 2016; Dong et al., 2016). High resolution stalagmite $\delta^{18}O$ records with accurate dating have indicated that climate change is closely related to the rise and fall of ancient dynasties (Zhang et al., 2008; Kathayat et al., 2017). However, the climatic interpretation of stalagmite $\delta^{18}O$ is still controversial (Pausata et al., 2011; Tan, 2014；Chen et al., 2015; Chiang et a l., 2020; Liu et al., 2020). In addition, there are still controversies about the climate change during the Xia and Shang Dynasties (Zhang et al., 2008; Lawler et al., 2009; Wu et al., 2016). Therefore, compared stalagmite $\delta^{18}O$, the high-resolution stalagmite multi-proxies records is better to reconstruct regional hydrological environment. Accurate reconstruction of the Paleoclimate will also contribute to the study of the evolution of human society (Kathayat et al., 2017; Zhang et al., 2018; Cheng et al., 2019).

2. Study Area and Sample

Yangkou Cave (29°02′N, 107°11′E) is located in southwest China, specifically in Mount Jinfo of Nanchuan and near the city of Chongqing (Fig. 1). The study site is located on the southeastern margin of the Sichuan Basin, along the northern margin of the Yun-Gui Plateau and at the northern end of the Dalou Mountains. The uppermost rock unit that makes up Mount Jinfo is Permian limestone, and a huge and complex underground cave system has developed within this unit (Zhang et al., 1998). The cave occurs at an elevation of 2140 m and is 2245 m in length and displays a corridor plane

https://doi.org/10.5194/cp-2021-20
Preprint. Discussion started: 15 March 2021

Climate of the Past Discussions

form. The width is generally 15–20 m, and the height is generally 8–12 m. The regional climate is influenced by both the Indian summer monsoon (ISM) and East Asian summer monsoon (EASM) (Fig. 1, Li et al., 2014). The regional annual mean temperature and annual precipitation is 8.5 °C and 1400 mm, respectively. Precipitation occurs primarily from April to October, when 83% of the annual precipitation occurs, and the annual mean temperature in the cave is 7.5 °C (Zhang et al., 1998; Li et al., 2014; Chen and Li, 2018). All the abbreviations in this study are listed in Table 1.

The stalagmite YK1306 without the top was collected exploring caves, and it was cut along the growth axis. Its profile is brown (Figure 2A). The diameter of the bottom of the stalagmite is about 80 mm, the diameter of the top is about 75 mm, and the length of the growth axis is 210 mm.

3. Methods

Parallel to the growth layers in stalagmite YK1306, powder sub-samples (5–20 mg) were collected from the polished profile of the stalagmite using a dental drill with a diameter of 1 mm for the U-Th age testing. A total of 11 dating samples were collected from stalagmite YK1306, respectively. The sampling locations are shown in Fig. 2A. The U and Th were separated using the standard chemical procedures described by Edwards et al. (1987) and Cheng et al. (2013). The ^{230}Th age of stalagmite YK1306 was determined in the Isotope Laboratory of the Institute of Global Environmental Change, Xi'an Jiaotong University using a multi-collector inductively coupled plasma mass spectrometer (MC-ICP-MS, Neptune-Plus). Uncertainties in U-Th isotopic data were calculated offline at the 2σ level, including corrections for blanks, multiplier dark noise, abundance sensitivity, and contents of the same nuclides in the spike solution (Cheng et al., 2013). The decay constant of ^{230}Th is 9.1705×10^{-6} yr^{-1} (Cheng et al., 2013), that of ^{234}U is 2.82206×10^{-6} yr^{-1} (Cheng et al., 2013), and that of ^{238}U is 1.55125×10^{-10} yr^{-1} (Jaffey et al., 1971). The corrected ^{230}Th ages assume an initial ^{230}Th/^{232}Th atomic ratio of $(4.4 \pm 2.2)\times10^{-6}$. These are the values for material in secular equilibrium with the bulk Earth ^{232}Th/^{238}U value.

The isotope sub-samples were collected using a dental drill from the polished profile along the central growth axis of the stalagmite at intervals of 0.25 mm (Fig. 2A). $\delta^{18}O$ and $\delta^{13}C$ were determined by phosphoric-acid reaction at 70ºC in an automated carbonate preparation device coupled to a Perspective IS mass spectrometer (Nu instrument) at the Beijing Createch Testing Technology Co., Ltd, China. $\delta^{18}O$ and $\delta^{13}C$ were corrected with internal and external standards, and precision is better than 0.08‰ and 0.06‰, respectively. Values are reported as per mil (‰) deviations from the Vienna Pee Dee Belemnite (V-PDB) standard.

Parallel to the isotope sampling path, trace element samples were scraped along the central axis with a 1 mm diameter dental drill. One sample every 1 mm were scraped from 0 to 30 mm (depth), and two samples every 1 mm were scraped from 30 to 65 mm (depth), with an average weight of 11 mg. After cleaning the PFA beaker, volumetric flask and centrifuge tube, soak them in 5% HNO_3 for 24 h, then rinse them with ultrapure water, and air-dry them. The sample were completely dissolved with 2 N HNO_3 in PFA beaker, transferring the dissolved solution to a 10 ml volumetric flask,

https://doi.org/10.5194/cp-2021-20
Preprint. Discussion started: 15 March 2021

then rinse PFA beaker twice with a small amount of ultrapure water, and the washed solution was transferred into the same volumetric flask. Next, the constant volume was 10 ml with ultrapure water. Finally, the solution in the volumetric flask was transferred into the centrifuge tube. The concentrations of cations Ca, Mg, Ba, and Sr were measured with the Optima 2100DV Inductively Coupled Plasma Emission spectrometer (ICP-OES) in Southwest University. The detection limit was 1 μg/L, and the analytical error was ≤2%.

4. Results

4.1 Chronology

The dating results are shown in Table 2. ^{238}U content is between 9365–25579 ppb, and ^{232}Th content is between 10–1452 ppt. High ^{238}U and low ^{232}Th content, yield precise dating results. The all dating errors are between 10 and 20 yr, and the average dating error is 15 yr. Based on the dating results, the chronology (Constructing Proxy Records from Age) is established in Modage software (Hercman et al., 2012). The results showed that the stalagmites deposited in 5040–2920 yr BP from 70 to 0 mm of distance from top.

4.2 Stable isotopes of Oxygen and Carbon

A total of 272 stable isotope have been analyzed, with an average resolution of 7 years. The maximum value of δ^{18}O is –6.4‰, the minimum value is –9.1‰, and the

https://doi.org/10.5194/cp-2021-20
Preprint. Discussion started: 15 March 2021

Climate of the Past
Discussions
Open Access

average value is –8.2‰; the maximum value of $\delta^{13}C$ is –1.4‰, the minimum value is –7.0‰, and the average value is –5.6 ‰. The $\delta^{18}O$ and $\delta^{13}C$ change synchronously (Fig. 3A and B). There was a significant correlation between $\delta^{18}O$ and $\delta^{13}C$ (R=0.95, n =272, P <0.01). The $\delta^{18}O$ and $\delta^{13}C$ values during 4600–4330 yr BP (58.5–54.5 mm) and 4070–3700 yr BP (42.5–30.5 mm) are significantly heavy than the values during 4330–4070 yr BP (54.5–42.5 mm) (Fig. 3 and Fig. S1). The maximum variation amplitudes of $\delta^{18}O$ and $\delta^{13}C$ are 2.7 ‰ and 5.6 ‰, respectively.

4.3 Trace element

The maximum Ca content is 632279 ppm, the minimum is 200909 ppm, the average is 300742 ppm; the maximum Mg content is 10061 ppm, the minimum is 1231 ppm, the average is 2902 ppm; the maximum Sr content is 12897 ppm, the minimum is 3355 ppm, the average is 5562 ppm; the maximum Ba content is 235 ppm, the minimum is 75 ppm, the average is 114 ppm. Ba/Ca, Sr/Ca, Mg/Ca covary with depth (Fig. S1). There is a significant correlation between Ba/Ca, Mg/Ca and Sr/Ca (Table S1). In order to better evaluate the information of hydrological environment change in four trace elements in stalagmite, we standardized Ba/Ca, Sr/Ca, Mg/Ca and analyzed Principal component analysis (PCA) in Matlab. The variance of principal components (PC) are shown in Table 3. The variance of PC1 is 67.15% (Table 3). Therefore, we chose PC1 as the variable representing Ba/Ca, Sr/Ca, Mg/Ca and compared it with $\delta^{18}O$ and $\delta^{13}C$ (Fig. 3 and Fig. S1). There was significant correlation between PC1 and $\delta^{13}C$, $\delta^{18}O$, Ba/Ca, Sr/Ca, Mg/Ca (Table S1). When the $\delta^{18}O$ and $\delta^{13}C$ were heavier during 4600–

https://doi.org/10.5194/cp-2021-20
Preprint. Discussion started: 15 March 2021

4330 and 4070–3700 yr BP, the increased PC1 indicates the increase of these trace elements. During 4330–4070 yr BP, $\delta^{18}O$ and $\delta^{13}C$ were lighter, and the decreased PC1 indicates the decrease of these trace elements. The correlation of these proxies is shown in Table S1.

5. Discussion

5.1 Interpretation of proxies

At present, most researches on stalagmites are based on stalagmite $\delta^{18}O$ to reconstruct paleoclimate change (Cheng et al., 2009, 2020; Kathayat et al., 2018; Zhang et al., 2018; Tan et al., 2020). Liu et al. (2015) and Chen et al. (2016) compared the stalagmite $\delta^{18}O$ records in the ASM region, indicating that the stalagmite $\delta^{18}O$ records showed the consistent changes from Centennial to the orbital scale. However, the instrumental data showed that the precipitation has the spatial difference between the north and the south in ASM region. As a result, the interpretation of stalagmite $\delta^{18}O$ is still controversial (Pausata et al., 2011; Tan, 2014； Chen et al., 2015; Liu et al., 2015; Chen et al., 2016; Chiang et a l., 2020; Liu et al., 2020). The reason for the controversy is that stalagmite $\delta^{18}O$ is not only affected by the intensity of the ASM (Wang et al., 2001), but also affected by the moisture sources and the pathway (Tan, 2014; Zhang and Li, 2019), upstream rainout (Baker et al., 2015; Liu et al., 2015; Li 2018), upstream convective activity (Baker et al., 2015; Liu et al., 2015; Li 2018), cloud height and temperature (Cai et al., 2016), westerlies (Chiang et a l., 2020) etc. However，Part of

https://doi.org/10.5194/cp-2021-20
Preprint. Discussion started: 15 March 2021

Climate of the Past Discussions

the controversy arises from differences in our understanding and the definition of monsoon intensity (Cheng et al., 2019). In addition, these debates mainly focus on interannual to interdecadal scale. The stalagmite $\delta^{18}O$ can reflect the intensity of ASM rather than precipitation on centennial to millennial scale (Tan et al., 2018; Cheng et al., 2019; Zhang et al., 2020). Moreover, the study of stalagmite multi-proxies can reliably reflect the changes of hydrological environment in the past (Fairchild et al., 2009; Tan et al., 2018; Zhang et al., 2018; Warken et al., 2018).

Compared with the $\delta^{18}O$ records of stalagmites, the $\delta^{13}C$ records are more sensitive to the changes in the ecological environment outside the cave (Zhang et al., 2015; Liu et al., 2016; Asmerom et al., 2020). The $\delta^{13}C$ of speleothems is affected by atmospheric CO_2, soil, vegetation, epikarst zone, and cave conditions (temperature, humidity, ventilation) (Li et al., 2018). Modern monitoring results show that the $\delta^{13}C$ in dripping water is controlled by surface precipitation, temperature and the CO_2 in soil, resulting in heavier $\delta^{13}C$ values in winter and spring and lighter $\delta^{13}C$ values in summer and autumn (Li and Li, 2018). The decrease of ASM and regional precipitation result in a decrease in vegetation coverage and soil microbial activity (Li et al., 2017). Then, the productivity of CO_2 in the soil from respiration and organic decomposition was reduced, the dripping speed slowed, and the degassing of the CO_2 in the epikarst zone increased, which increased the $\delta^{13}C$ values of the speleothems (Tan et al., 2015; Li et al., 2018; Zhao et al., 2020).

Mg/Ca, Ba/Ca and Sr/Ca of stalagmite have been used as indicators of regional hydrological environment (Fairchild et al., 2009; Griffiths et al., 2010; Liu et al., 2013;

https://doi.org/10.5194/cp-2021-20
Preprint. Discussion started: 15 March 2021

Climate of the Past Discussions

Zhang et al., 2018). Modern cave monitoring provides reliable evidence that Mg/Ca, Ba/Ca and Sr/Ca co-vary (Warken et al., 2018). When the regional precipitation decreased, the CO_2 degassing and prior calcite precipitation (PCP) increased in the epikarst zone, resulting in an increase in the Mg/Ca, Ba/Ca and Sr/Ca ratios of the stalagmites (Liu et al., 2013; Chen and Li, 2018; Zhang et al., 2018; Warken et al., 2018; Carolin et al., 2019). Our monitoring in YK cave also showed that the precipitation decreased, the Mg/Ca and Sr/Ca in the cave drips increased; and as the precipitation increased, the Mg/Ca and Sr/Ca decreased (Chen and Li, 2018). Therefore, PC1 as a common variable of Mg/Ca, Ba/Ca and Sr/Ca, the high value of PC1 represents dry and the low value represents wet.

5.2 The structure and driving mechanism of 4.2 ka event

5.2.1 4.2 ka event recorded by multi-proxies in stalagmite YK1306

The $\delta^{18}O$ record of stalagmite YK1306 indicates that the ASM weakened during 4600–4330 and 4070–3700 yr BP, but strengthened during 4330–4070 yr BP (Fig. 3 and 4A). This indicates that the ASM had three stages marked as I–II–III (Corresponding to weak-strong-weak) during the 4.2 ka event (Fig. 3 and 4A). The $\delta^{18}O$ and $\delta^{13}C$ of stalagmite YK1306 were significantly correlated (Table S1), and they changed synchronously (Fig. 3A and 3B). When the ASM decreased, precipitation and soil microbial activity decreased, soil CO_2 production decreased, and $\delta^{13}C$ is heavier; on the contrary, when the ASM and precipitation increased, then surface vegetation

https://doi.org/10.5194/cp-2021-20
Preprint. Discussion started: 15 March 2021

coverage and soil microbial activity increased, soil CO_2 production increased, ultimately, the $\delta^{13}C$ is lighter (Fig. 3A) (Zhao et al., 2020; Tan et al., 2015; Li et al., 2018). In addition, the change of Mg/Ca, Ba/Ca and Sr/Ca ratios responded quickly to the changes of local hydrological conditions (Fig. 3 and Fig. S1). The period of II stage, the value of PC1 decreased when ASM became stronger, indicating the humid environment in the region (Fig. 3). During I and III stage, the PC1 value increased when the ASM weakened, indicating the regional arid environment (Fig. 3). However, the amplitude of PC1 during I stage was small than the variation of PC1 during III stage (Fig. 3C). It may be that the ASM during III stage sustained longer and became weaker (Fig. 3).

5.2.2 Comparison of different geologic record and driving mechanism

A large amount of evidence showed that the 4.2 ka event affected global climate change (Bond et al., 2001; Tan et al., 2008; Berkelhammer et al., 2012; Kathayat et al., 2018; Ran and Chen, 2019). The 4.2 ka event also was recorded as stalagmites (Berkelhammer et al., 2012; Tan et al., 2018; Kathayat et al., 2018; Zhang et al., 2018), peat (Hong et al., 2003), lake sediments (Xiao et al., 2008, 2018), pollen (Park et al., 2019), loess (Zha et al., 2019) in the Asian monsoon region. Previous studies suggested that the ASM weakened during the 4.2 ka event and the EASM region became cold and dry climate (Tan et al., 2008; Berkelhammer et al., 2012; Xiao et al., 2018; Ran and Chen, 2019). Recent studies indicated that the south of the EASM region was humid during the 4.2 ka event (Tan et al., 2018; Zhang et al., 2018). However, These studies

https://doi.org/10.5194/cp-2021-20
Preprint. Discussion started: 15 March 2021

Climate of the Past Discussions

revealed that 4.2 ka event only have a unimodal structure. Therefore, the internal structure of the 4.2 ka event was still unclear (Xiao et al., 2018; Tan et al., 2020).

Multiple stalagmite $\delta^{18}O$ records in the ASM region showed that the ASM presented three stages (weak-strong-weak pattern) during the 4.2 ka event (Fig. S2). The $\delta^{18}O$ of the stalagmites from Xianglong Cave (XL), Jiuxian Cave (JX) and Wuya Cave (WY) in northern China, is similar to the structure of the $\delta^{13}C$ and $\delta^{18}O$ in stalagmite YK1306 (Fig. S2). The stalagmite $\delta^{18}O$ of Shennong Cave (SN) in southeast China also showed the same change (Fig. S2D). Although the stalagmite $\delta^{18}O$ of Dongge Cave (DG) in Southwest China fluctuated slightly during the II stage period, the structure of "weak-strong-weak" was still very significant during the whole 4.2 ka event (Fig. S2 B). The reproducibility of stalagmite records in different caves verifies the stalagmite YK1306 records, indicating consistent variation of ASM at that time on a large spatial scale (Fig. S2 and Fig. 4). The differences of duration and amplitude in three stages of these records may be attributed to the differences in dating error and resolution (Duan et al., 2014; Kathayat et al., 2018), and may also be related to the differences in regional hydrological environment and cave environment (Fairchild et al., 2009; Duan et al., 2014). For example, the resolution of stalagmite records in DG and WY Cave is higher, but their dating errors are more than 47 yr. The stalagmite records of SN Cave is shorter than others records and the stalagmite records in JX Cave lack of age control (Fig. S2). The stalagmite $\delta^{18}O$ in Sahiya Cave (SHY) also showed that the ISM appeared "weak-strong-weak" pattern during the 4.2 ka event (Fig. S2 G). The stalagmite $\delta^{18}O$ of GZ Cave and the Jeita Cave in the Middle East (Fig. 1) also

https://doi.org/10.5194/cp-2021-20
Preprint. Discussion started: 15 March 2021

indicated similar climate change pattern of "dry-wet-dry" during the 4.2 ka event (Fig. 4D and E) (Cheng et al., 2015; Carolin et al., 2019). However, clay content and Ti in ALake lake, which is dominated by westerly wind, indicated that WDCR presented a pattern (wet-dry-wet) opposite to that of ASM during the 4.2 ka event (Fig. 4B). The above discussion revealed that the EASM, ISM and Middle East region' climate show similar change patterns during the 4.2 ka event, while WDCR is opposite. Hence, it may be driven by the same driving mechanism.

Previous studies have shown that the intensity of AMOC affects the variation of the global climate (Cheng et al., 2009；Zhang et al., 2018; Li et al., 2021). The content of Hematite-stained grains, indicating the intensity of AMOC, showed that the ice debris with the double peak poured into the North Atlantic during the 4.2 ka event (Fig. 5B) (Bond et al., 2001). The Greenland temperature synchronous decreased during I and III stage (Fig. 5A). A large amount of fresh water injected into the North Atlantic, resulting in the weakening of AMOC (Cheng et al., 2009；Zhang et al., 2018). The simulation results also showed that the AMOC intensity was "weak-strong-weak" during the 4.2 ka event (Yan and Liu, 2019; Ning et al., 2019; Li et al., 2021). Yan and Liu (2019) used the trace-21ka simulations to show that the two centennial scale positive NAO-like are closely related to the structure of the 4.2 ka event. NAO could trigger circular Global Telecommunication (CGT) connecting climate change at high and low latitudes (Huang et al., 2015; Yan and Liu, 2019). In positive NAO-like, Azores high and westerly wind strengthen, which restrain the intensity of ASM or vice versa (Chiang et al., 2020; Li et al., 2021). A negative height anomalies in Central Asia and

https://doi.org/10.5194/cp-2021-20
Preprint. Discussion started: 15 March 2021

positive height anomalies in the Mediterranean Sea and North China, leading to strengthened meridional winds in the westerlies-dominated climatic regime (Huang et al., 2015; Chen et al., 2019). This brings more water vapor from the Indian Ocean and Arabian Sea, and subsequently increases precipitation in the region (Huang et al., 2015; Chen et al., 2019). Therefore, the precipitation pattern in the WDCR is opposite to that in the ASM region (Fig. 4A-B). Moreover, dust storms in northern China increased significantly when ASM decreased (Chen et al., 2020; Peng et al., 2021). Yuexi peatland in Southwest China recorded that the dust flux from northern China increased significantly during the I and III stages (weak ASM) during the 4.2 ka event (Fig. 4C). Similarly, in the two droughts during the 4.2 ka event, the stronger wind brought dust flux from Mesopotamia region (Fig. 4D) (Carolin et al., 2019).

In addition, the stalagmite $\delta^{18}O$ of LL Cave in Flores island, south of the equator, indicated a pattern opposite to that of the ASM during the 4.2 ka event (Fig. 1, Fig. 4F). AISM presented three stages of "strong-weak-strong" (Griffiths et al., 2010). The results of trace-21ka simulations also proved the opposite change pattern in the northern and southern Hemispheres (Yan and Liu, 2019). This is because the weakening of the AMOC will lead to the south shift of ITCZ (Cheng et al., 2009; Wang et al., 2017), which will strengthen the AISM in the southern Hemisphere (Griffiths et al., 2009; 2010). Therefore, AISM is opposite to ASM (Griffiths et al., 2009).

5.2.3 The structure of 8.2 ka event is similar to that of 4.2 ka event

The 4.2 ka and 8.2 ka events affected global climate change in the Holocene

https://doi.org/10.5194/cp-2021-20
Preprint. Discussion started: 15 March 2021

(Cheng et al., 2009; Daley et al., 2011; Berkelhammer et al., 2012; Ran et al., 2019). When the Laurentine ice sheet melted with the increase of solar radiation in Holocene, the remaining ice sheet occupied Huddson Strait and formed AOL lake (Barber et al., 1999). The most records suggested that the AOL lake burst suddenly at 8470±300 yr BP, resulting in 8.2 ka event (Alley et al., 1997; Barber et al., 1999; Kobashi et al., 2007; Cheng et al., 2009; Daley et al., 2011). A large amount of fresh water injected into the North Atlantic, resulting in the decrease of AMOC, which eventually led to the weak the ASM and strong South American Summer Monsoon (Cheng et al., 2009). Daley et al. (2011) thought that after the AOL lake burst, fresh water had two pulse injection and continuously injected into the North Atlantic through the Hudson Strait, resulting in the bimodal structure of the 8.2 ka event. However, some studies suggested that the the dating estimating of the collapse time of AOL lake is still rough (Li et al., 2012). Sea level records in the Mississippi River Delta suggested that the injection may be transient rather than a long-term recharge (Li et al., 2012). Therefore, what caused the bimodal structure of the 8.2 ka event is still a puzzle.

The comparison between the stalagmites of DG, WY in the EASM region and the Qunf Cave stalagmite in the ISM region showed that the ASM also divided into three stages of “weak-strong-weak” pattern during the 8.2 ka event (Fig. 6) (Cheng et al., 2009; Tan et al., 2020). This structure of the 8.2 ka event is a common in the northern Hemisphere during, which is opposite to that in the southern Hemisphere (Cheng et al., 2009). This indicates that the 4.2 ka and 8.2 ka events have similar change structures (Fig. 4 and Fig. 6). Therefore, the two events may be dominated by the common climate

https://doi.org/10.5194/cp-2021-20
Preprint. Discussion started: 15 March 2021

driving mechanism. The AMOC and the phase of NAO modulated the hemispherically symmetric forcings (Geirsdóttir et al., 2019).

5.3 The relation between floods and drought climate and ancient civilization during 4.2 ka event

Due to the lack of documentary, the exact time of the origin of Xia Dynasty of the first dynasty in ancient China, is still uncertain (Wu et al., 2005; Lawler, 2009). Now, the government thought that the Xia Dynasty was established at ~4070 yr BP (Wu et al., 2016; Dong et al., 2018). It is said that Dayu won the support of various tribes because he succeed in controlling floods, established the Xia Dynasty and was the first emperor (Wu et al., 2005). The historians speculated that there were flood disaster before the establishment of the Xia Dynasty (Lawler et al., 2009; Wu et al., 2016). The flood may also lead to the fall of Longshan Culture in northern China and Liangzhu Culture in southern China (Shi et al., 1992). However, due to the lack of accurate historical data, accurate dating and high-resolution paleoclimate records, the time and cause of the floods are questionable (Wu et al., 2005; Wu et al., 2016; Xiao et al., 2018). Therefore, the study of the time and cause of the flood is conducive to prove the origin of the Xia Dynasty.

Wu et al. (2016) suggest that the earthquake led to the formation of Jishi Gorge barrier lake in the upper reaches of the Yellow River, and then the collapse of the barrier lake led to the flood in the Yellow River Basin at 3870 yr BP. As a result, Xia Dynasty was established at 3850 yr BP (Wu et al., 2016). However, the dating of the Lajia

https://doi.org/10.5194/cp-2021-20
Preprint. Discussion started: 15 March 2021

Climate of the Past Discussions

cultural site in the lower reaches of Jishi Gorge barrier lake showed that Jishi Gorge barrier lake was extinct as early as 5600 yr BP (Dong et al., 2018). The time of the earthquake is later than 3800 yr BP (Dong et al., 2018; Huang et al., 2019). There is no sedimentary layer of collapse in the lower Yellow River (Huang et al., 2019). Therefore, the origin of Xia Dynasty at 3850 yr BP may not be accurate.

The palaeoflood Slackwater deposits (SWD) in the loess profile of Qishui (QS) river side (the Yellow River Basin) indicated that floods occurred during 4300–4000 yr BP (Huang et al., 2011). The SWD in Hanjiang River (HJ) side (a tributary of the Yangtze River) showed that the floods occurred in 4200–4000 yr BP (Fig. 7E) (Liu et al., 2015). The SWDs of QS and HJ were deposited on the Longshan cultural layer and Shijiahe cultural layer, respectively (Fig. 7D and 7E). However, the accuracy of this age of SWDs were larger with an error of 180–340 yrs (Fig. 7D and 7E) (Huang et al., 2011; Liu et al., 2015). In short, there is no doubt that there was great flood during the 4.2 ka event, which may lead to the fall of Longshan culture and Liangzhu culture (Gao et al., 2005; Huang et al., 2011).

The $\delta^{18}O$ of stalagmite YK1306 indicated that the ASM was strong during 4330–4070 yr BP (Fig. 7A), and the precipitation in northern China increased (Fig. 7C). The $\delta^{13}C$, Ba/Ca, Sr/Ca, Mg/Ca of stalagmite YK1306 indicated that the Yangtze River Basin was also a humid period (Fig. 3 and Fig. 4). Therefore, the floods may be caused by strong ASM and occurred during 4330–4070 yr BP. The Bamboo Annals recorded that the leaders (Yao and Shun) of tribes before Dayu started flood control, the period of floods could continue for at least 150 years (Wu et al., 2005). Therefore, floods

https://doi.org/10.5194/cp-2021-20
Preprint. Discussion started: 15 March 2021

Climate of the Past Discussions

occurred frequently before the establishment of the Xia Dynasty, rather than instantaneous outburst. The stalagmite YK1306 indicated that ASM became stronger during II stage (Fig. 7A), supporting this deduction. After 4070 yr BP, the ASM decreased (Fig. 7A) and the precipitation in the ASM region decreased (Fig. 3 and Fig. 4), which may end the floods. Therefore, under the condition of relatively backward production technology, the main reason for Dayu's successful flood control may be the ASM and the precipitation decreased. This indirectly showed that Dayu lived around 4070yr BP (Fig. 7A), and the current government thought that the Xia Dynasty began at 4070 yr BP is reliable. According to our research, it is supported that the end of Shijiahe culture and Liangzhu Culture in the Yangtze River basin may be caused by frequent floods (Fig. 7B) (Gao et al., 2005; Chen et al., 2018). In addition, the extremely dry climate could trigger social unrest (Fang et al., 2015; Kathayat et al., 2017). The fall of Qujialing culture, Xia Dynasty and Shang Dynasty may be related to the drought climate (Fig. 7B).

6. Conclusions

In this study, we used the multi-proxies of stalagmite YK1306 of YK cave in southwestern China to reconstruct the variation of ASM during 5000–3000 yr BP. The $\delta^{13}C$ and $\delta^{18}O$ were heavy and Ba/Ca, Sr/Ca, Mg/Ca ratios increased during 4600–4330 yr BP and 4070–3700 yr BP, indicating that the ASM weakened and precipitation decreased. During 4330–4070 yr BP, $\delta^{13}C$ and $\delta^{18}O$ were lighter and Ba/Ca, Sr/Ca, Mg/Ca ratios decreased, the ASM strengthened, and precipitation increased. The multi-

https://doi.org/10.5194/cp-2021-20
Preprint. Discussion started: 15 March 2021

proxies of stalagmite YK1306 showed that the ASM had three stages of "weak-strong-weak" during the 4.2 ka event, which reappeared in different geologic records. The differences of duration and amplitude in three stages of the records in the northern and southern Hemispheres may be attributed to the differences in dating error and resolution. However, westerlies and AISM both showed the opposite change pattern (strong-weak-strong) with the ASM. The two centennial scale positive NAO-like are closely related to the structure of the 4.2 ka event. In positive NAO-like, Azores high and westerly wind strengthen, which restrain the intensity of Asian summer monsoon or vice versa. Thus, the ASM region and the Middle East region showed bimodal drought during the 4.2 ka event and there were increase in dust flux from the north in both regions. The strengthened meridional winds in the WDCR, leading to more water vapor from the Indian Ocean and Arabian Sea, and subsequently increases precipitation in the WDCR. Meanwhile, the weak AMOC will lead to the south shift of ITCZ and strengthen the AISM in the southern Hemisphere, which is opposite to ASM. The structure of "weak-strong-weak" pattern of the ASM during the 8.2 ka event was similar to that of the 4.2 ka event. Therefore, the two events may be driven by the same mechanism. In addition, the strong ASM may have led to the frequent occurrence of ancient floods on the eve of the Xia Dynasty, which led to the fall of Longshan culture and Liangzhu culture. The weak ASM after 4070 yr BP was one of the truth reasons of Dayu's successful regulating of floodwaters. The fall of Qujialing culture, Xia Dynasty and Shang Dynasty may be related to the drought climate. Of course, more high-resolution reconstruction of paleoclimate and investigation of human civilization sites in the future

https://doi.org/10.5194/cp-2021-20
Preprint. Discussion started: 15 March 2021

Climate of the Past Discussions

will contribute to the origin of Xia Dynasty and the evolution of civilization.

Data availability.

Research data from this study are available on request (cdlity@163.com).

Author Contributions

C.-J. Chen, T.-Y Li and J. -Y. Li designed the research and revised the manuscript. C.-J. Chen wrote the first version of the manuscript. D.-X. Yuan and X.-F Wang improved manuscript quality. Y. Wu, S.-Y. Xiao, Y.-Z Xu, Y.-Y Huang, H.-Y Qiu, and M.-Q Liang contributed to oxygen isotope measurements and the ^{230}Th dating work. H. Cheng, Y.-F Ning and R. Lawrence Edwards provided technical support in ^{230}Th dating work. All authors discussed the results and provided ideas to input the manuscript.

Competing interests

The authors declare no competing interests.

Acknowledgements

This research was supported by the National Natural Science Foundation of China (NSFC, No. 41772170; 42011530078), and the Fundamental Research Funds for the Central Universities, China (No. XDJK2017A010) to T.-Y. Li, and the Chongqing Municipal Science and Technology Commission Fellowship Fund (no. cstc2018jcyj-

https://doi.org/10.5194/cp-2021-20
Preprint. Discussion started: 15 March 2021

Climate of the Past Discussions

yszx0013) to D.-X Yuan. The Open Project of Guangxi Key Science and Technology Innovation Base on Karst Dynamics (KDL & Guangxi 202003) to J.-Y. Li. This research was supported by the China Scholarship Council (CSC) to C.-C. Chen (202006990068). We also thank professor Y.-J Jiang, B.-Y Wang, and R. Zhang of Southwest University for meaningful suggestions.

References

Alley, R.B., Mayewski, P. A., Sowers, T., Stuiver, M., Taylor, K. C., Clark, P.U.: Holocene climatic instability: a prominent, widespread event 8200 yr ago, Geology., 25, 483–486, 1997.

Asmerom, Y., Baldini, J.U.L., Prufer, K.M., Polyak, V.J., & Kennett, D.J.: Intertropical convergence zone variability in the Neotropics during the common Era, Sci. Adv., 6, https://doi.10.1126/sciadv.aax3644, 2020.

Barber, D.C., Bilodeau, G., Southon, J., M.D. Morehead, Kerwin, M.W., & Mcneely, R., et al.: Forcing of the cold event of 8,200 years ago by catastrophic drainage of Laurentide lakes, Nature., 400, 344–348, 1999.

Berkelhammer, M., Sinha, A., Stott, L., Cheng, H., Pausata, F.S., Yoshimura, K.: An abrupt shift in the Indian monsoon 4000 years ago, Geophys. Monogr. Ser, 198, 75–87, 2012.

Bond, G.C., Kromer, B., Beer, J., Muscheler, R., & Bonani, G.: Persistent solar influence on north Atlantic climate during the Holocene, Science., 294, 2130–2136, 2001.

Briner, J.P., Cuzzone, J.K., Badgeley, J.A., Nicolás E. Young, & Nowicki, S.: Rate of mass loss from the greenland ice sheet will exceed Holocene values this century, Nature., 586, 70–74. 2020.

Cai Z, Tian L. Atmospheric Controls on Seasonal and Interannual Variations in the Precipitation isotope in the East Asian Monsoon region, J. Climate., 29, 1339–1352, 2016.

Carolin, S.A., Richard, T.W., Christopher, C.D., Vasile, E., R. Alastair, S., Michael, W D., Morteza, T., Gideon, M.H.: Precise timing of abrupt increase in dust activity in the middle east coincident with 4.2 ka social change, Proc. Natl. Acad. Sci.,116, 67–72, 2019.

Chen, C.-J., Li, T.-Y. Geochemical characteristics of cave drip water respond to ENSO based on a 6-year monitoring work in Yangkou Cave, Southwest China, J. Hydrol., 561, 896–907, 2018.

Chen, F., Xu, Q., Chen, J., Birks, H. J. B., Liu, J., Zhang, S., Jin, L., An, C., Telford, R. J., and Cao, X.: East Asian summer monsoon precipitation variability since the last deglaciation, Sci. Rep., 5, 11186, https://doi.org/10.1038/srep11186, 2015.

Chen, F., Chen, J., Huang, W., Chen, S., Huang, X., & Jin, L.: Westerlies Asia and monsoonal Asia: spatiotemporal differences in climate change and possible mechanisms on decadal to sub-orbital timescales. Earth-Sci. Rev., 192, 337–354, 2019.

Chen, F.H., Chen, S.Q., Zhang, X., Chen, J.H., Wang, X., Gowan, E.J., Qiang, M.R., Dong, G.H., Wang, Z.L., Li, Y.C., Xu, Q.H., Xu, Y.Y., Smol, J.P., Liu, J.B.: Asian dust-storm activity dominated by Chinese dynasty changes since 2000 BP, Nat. Commun., 11, https://doi.10.1038/s41467-020-14765-4, 2020.

Chen, J.H., Rao, Z.G., Liu, J.B., Huang, W., Feng, S., Dong, G.H., Hu,Y., Xu, Q.H., Chen, F.H.: On the timing of the East Asian summer monsoon maximum during the Holocene—Does the speleothem oxygen isotope record reflect monsoon rainfall variability?, Sci. China Earth Sci., 59, 2328–2338, 2016.

Chen, R., LI, F.Q.,Wang, T.Y., Li, D., Wei, Y., Zhou, G.H.: The size distribution of Neolithic sites in the middle reaches of the Yangtze River, A. Geograph. Sinica., 73, 474–486, 2018. (in Chinese with English abstract)

Cheng H, Edwards R.L, Shen C.C, Polyak V.J, Asmerom Y, Woodhe A.D.J, Hellstrom J, Wang Y, Kong X, Spötl C.: Improvements in ^{230}Th dating, ^{230}Th and ^{234}U half-life values, and U-Th isotopic measurements by multi-collector inductively coupled plasma mass spectroscopy, Earth Planet. Sci. Lett., 371, 82–91, 2013.

Cheng, H., Fleitmann, D., Edwards, R. L., Wang, X., Cruz, F.W., & Auler, A.S.: Timing and structure of the 8.2 kyr BP event inferred from δ^{18}O records of stalagmites from China, Oman, and Brazil, Geology., 37, 1007–1010, 2009.

Cheng, H., Zhang, H., Spol, C., Baker, J., &Edwards, R.L.: Timing and structure of the younger dryas event and its underlying climate dynamics, Proc. Natl. Acad. Sci., 117, https://doi.10.1073/pnas.2007869117, 2020.

https://doi.org/10.5194/cp-2021-20
Preprint. Discussion started: 15 March 2021

Cheng, H., Zhang, H., Zhao, J., Li, H., Ning, Y., Kathayat, G.: Chinese stalagmite paleoclimate researches: A review and perspective. Sci. China Earth Sci., 1–25, 2019.

Chiang, J. C. H., Herman, M. J., Yoshimura, K., & Fung, I. Y.: Enriched east Asian oxygen isotope of precipitation indicates reduced summer seasonality in regional climate and westerlies, Proc. Natl. Acad. Sci., 117, https:// 10. 1073/pnas.1922602117, 2020.

Daley, T.J., Thomes, E.R., Holmes, J.A., Chapman, M.R., Tindall, J. Robertson, I. :The 8200 yr BP cold event in stable isotope records from the North Atlantic region, Global planet. Change., 79, 288-302, 2011.

Dong, G.H., Zhang, F.Y., Liu, F.W., Zhang, D.J., Zhou, A.F., Yang, Y.S., Wang, G.H.: Multiple evidences indicate no relationship between prehistoric disasters in Lajia site and outburst flood in upper Yellow River valley, China, Sci. China Earth Sci., 61: 441–449, 2018.

Duan, F., Wang, Y., Shen, C. C., Wang, Y., Cheng, H., & Wu, C. C.: Evidence for solar cycles in a late Holocene speleothem record from Dongge cave, China, Sci. Rep., 4, https://doi.10.1038/srep05159, 2014.

Edwards R.L, Chen J.H, Wasserburg G J.: ^{238}U-^{234}U-230Th-^{232}Th systematics and the precise measurement of time over the past 500,000 years, Earth Planet. Sci. Lett., 81, 175–192, 1987.

Fairchild, I.J., Treble, P.C.: Trace elements in speleothems as recorders of environmental change, Quat. Sci. Rev., 28, 449–468, 2009.

Fang, X.Q., Su, Y., Yin, J., Teng, J.C.: Transmission of climate change impacts from temperature change to grain harvests, famines and peasant uprisings in the historical China, Sci. China Earth Sci., 45, 831–842. 2015.

Fleitmann, D., Burns, S.J., Mudelsee, M., Neff, U., Kramers, J., Mangini, A., and Matter, A.: Holocene forcing of the Indian Monsoon recorded in a stalagmite from southern Oman, Science., 300, 1737–1739, 2003.

Gao, M.H. The Ecological System and the Relationship Between Human and Environment in the Process of Civilization, Fudan J. (Social Sci. Edtion)., 139, 128–134, 2005. (in Chinese)

Geirsdóttir, Á., Miller, G.H., Andrews, J.T., Harning, D.J., Anderson, L.S., Florian, C., Larsen, D.J., and Thordarson, T.: The onset of neoglaciation in Iceland and the 4.2 ka event, Clim. Past., 15, 25–40, 2019.

https://doi.org/10.5194/cp-2021-20
Preprint. Discussion started: 15 March 2021

Griffiths, M.L., Drysdale, R.N., Gagan, M.K., Frisia, S., Zhao, J.X., & Ayliffe, L.K.: Evidence for Holocene changes in Australian–Indonesian monsoon rainfall from stalagmite trace element and stable isotope ratios, Earth Planet. Sci. Lett., 292, 27–38, 2010.

Griffiths, M.L., Drysdale, R.N., Gagan, M.K., Frisia, S., Zhao, J.X., & Ayliffe, L.K.: Evidence for Holocene changes in Australian–Indonesian monsoon rainfall from stalagmite trace element and stable isotope ratios, Earth Planet. Sci. Lett., 292, 27–38, 2010.

Griffiths, M.L., Drysdale, R.N., Gagan, M.K., Zhao, J.X., & Suwargadi, B.W.: Increased Australian–Indonesian monsoon rainfall linked to early Holocene sea-level rise, Nat. Geosci., 2, 636–639, 2009.

Hercman H, Pawlak J.: MOD-AGE: An age-depth model construction algorithm, Quat. Geochronol., 12, 1–10, 2012.

Hong, Y.T., Hong, B., Lin, Q.H., Zhu, Y.X., Shibata, Y., & Hirota, M.: Correlation between Indian ocean summer monsoon and North Atlantic climate during the Holocene, Earth Planet Sci. Lett., 211, 371–380, 2003.

Huang, C. C., Pang, J., Zha, X., Su, H., & Jia, Y.: Extraordinary floods related to the climatic event at 4200 a BP on the Qishuihe river, middle reaches of the yellow river, China. Quat, Sci. Rev., 30, 460–468, 2011.

Huang, C.C., Guo, Y.Q., Zhang, Y.Z., Zhou, Y.L., Zhao, H., Zheng, Z.X, Zhou, Q., Pang, J.L., Wang, H.Y., Cuan, Y.D., Zha, X.C., Hu, G.M., Liu, T.: Holocene sedimentary stratigraphy and pre-historical catastrophes over the Lajia Ruins within the Guanting Basin in Qinghai province of China, Sci. China Earth Sci., 49, 434–455. 2019.

Huang, W., Feng, S., Chen, J., Chen, F.: Physical Mechanisms of Summer Precipitation Variations in the Tarim Basin in Northwestern China, J. Climate., 28, 3579–3591, 2015.

Jaffey A H, Flynn K F, Glendenin L E, Bentley W C, Essling A M. Precision measurement of half-lives and specific activities of ^{235}U and ^{238}U, Phys. Rev., 4, 1889–1906, 1971.

Jiang, H., Muscheler, R., Bjorck.: Solar forcing of Holocene summer sea-surface temperatures in the northern North Atlantic, Geology., 43, 203–206, 2015.

Kathayat, G., Cheng, H., Sinha A.: Evaluating the timing and structure of the 4.2 ka event in the Indian summer monsoon domain from an annually resolved speleothem record from Northeast India, Clim. Past., 14(12):1869–1879, 2018.

Kathayat, G., Cheng, H., Sinha, A., Yi, L., Li X., Zhang, H., Li, H., Ning, Y., Edwards R.L.: The Indian monsoon variability and civilization changes in the Indian subcontinent, Sci. Adv., 3, https://doi.10.1126/sciadv.1701296, 2017.

Kobashi, T., Menviel, L., Jeltsch-Thmmes, A., Vinther, B. M., Box, J.E., & Muscheler, R.: Volcanic influence on centennial to millennial Holocene Greenland temperature change, Sci. Rep., 7, https://doi.10.1038/s41598-017-01451-7, 2017.

Kobashi, T., Severinghaus, J.P., Brook, E.J., Barnola, J.M., & Grachev, A.M.: Precise timing and characterization of abrupt climate change 8200 years ago from air trapped in polar ice, Quat, Sci. Rev., 26, 1212–1222, 2007.

Lawler, & A.: Founding dynasty or myth?, Science., 325, 934–934, 2009.

Li J.-Y, Li H.-C, Li T.-Y, Mii H.-S, Yu T-L, Shen C.-C, Xu X.: High-resolution $\delta^{18}O$ and $\delta^{13}C$ records of an AMS ^{14}C and ^{230} Th/U dated stalagmite from Xinya Cave in Chongqing: Climate and vegetation change during the late Holocene, Quat. Int., 447, 75–88, 2017,

Li J.-Y, Li T.-Y.: Seasonal and annual changes in soil/cave air pCO_2 and the $\delta^{13}C$ DIC of cave drip water in response to changes in temperature and rainfall, Appl. Geochem., 93, 94–101, 2018.

Li T. -Y., Huang C.-X., Tian L., Suarez, M.B., Gao Y.: Variation of $\delta^{13}C$ in plant-soil-cave systems in karst regions with different degrees of rocky desertification in Southwest China and implications for paleoenvironment reconstruction, J. Cave Karst Stud., 80, 212–228, 2018.

Li T.-Y, Shen C.-C, Li H.-C, Li J.-Y, Chiang H.-W, Song S.-R, Wang J.-L.: Oxygen and carbon isotopic systematics of aragonite speleothems and water in Furong Cave, Chongqing, China. Geochim. Cosmochim. Acta., 75, 4140–4156, 2011a.

Li, Y., Han, L., Liu, X.q., Song, Y.G., Wang, Y.X.: Correlation and anti-correlation of the Asian summer monsoon and westerlies during the Holocene, Gondwana Res., 91, 112–120. 2021.

Liu, D., Wang, Y., Cheng, H., Edwards, R.L, Kong, X., Li T.Y.: Strong coupling of centennial-scale changes of Asian monsoon and soil processes derived from stalagmite $\delta^{18}O$ and $\delta^{13}C$ records, southern China, Quat. Res., 85, 333–346, 2016.

Liu, J., Chen, J., Zhang, X., Li, Y., & Chen, F.: Holocene east Asian summer monsoon records in northern china and their inconsistency with chinese stalagmite $\delta^{18}O$

https://doi.org/10.5194/cp-2021-20
Preprint. Discussion started: 15 March 2021

records, Earth-Sci. Rev., 148, 194–208, 2015.

Liu, T., Huang, C.C., Pang, J., Zha, X., Zhou, Y., & Zhang, Y.: Late Pleistocene and Holocene palaeoflood events recorded by slackwater deposits in the upper Hanjiang river valley, China, J. Hydrol., 529, 499–510, 2015.

Liu, Y.H., Henderson, G.M., Hu, C.Y., Mason, A.J., Charnley, N., Johnson, K.R., & Xie, S.C.: Links between the East Asian monsoon and North Atlantic climate during the 8200 year event, Nat. Geosci., 6(2), 117–120. 2013.

Nakamura, A., Yokoyama, Y., Maemoku, H., Yagi, H., Okamura, M., & Matsuoka, H. Weak monsoon event at 4.2 ka recorded in sediment from lake rara, Himalayas, Quat. Inter., 397, 349–359, 2016.

Ning, L., Liu, J., Bradley, R.S., & Yan, M.: Comparing the spatial patterns of climate change in the 9th and 5th millennia BP from trace-21 model simulations, Clim. Past., 15, 41–52, 2019.

Park, Jun., Park, Jin., Yi, San., Kim, J.C., Lee, E., Choi, J.: Abrupt Holocene climate shifts in coastal east Asia, including the 8.2 ka, 4.2 ka, and 2.8 k a BP events, and societal responses on the Korean Peninsula, Sci. Rep., 9, https://doi.10.1038/s41598-019-47264-8, 2019.

Pausata, F.S.R., Battisti, D.S., Nisancioglu, K.H., Bitz, C.M.: Chinese stalagmite $\delta^{18}O$ controlled by changes in the Indian monsoon during a simulated Heinrich event, Nat.Geosci., 4, 474–480, 2011.

Peng, H., Bao, K., Yuan, L., Uchida, M., Hong, Y.: Abrupt climate variability since the last deglaciation based on a high-resolution peat dust deposition record from southwest China, Quat. Sci. Rev., 252, https://doi.10.1016/j.quascirev.2020.106749, 2021.

Ran, M., & Chen, L.: The 4.2 ka BP climatic event and its cultural responses. Quat. Intern., 521,158–167, 2019.

Shi, Y.F., Kong, Z.C., Wang, S.M., Tang, L.Y., Wang, F.B., Yao, T.D.: Climate fluctuation and important events during the Great Warming period of Holocene in China, Sci. China Earth Sci., 12, 1300-1308,1992.

Tan L, Cai Y, An Z, Cheng H, Shen C.C, Breitenbach S.F, Du Y.: A Chinese cave links climate change, social impacts, and human adaptation over the last 500 years, Sci. Rep., 5, https://doi.10.1038/srep12284. 2015.

Tan, L., An, Z., Cai, Y., Long, H.: The hydrological exhibition of 4200 a BP event in

https://doi.org/10.5194/cp-2021-20
Preprint. Discussion started: 15 March 2021

Climate of the Past
Discussions
Open Access
EGU

China and its global linkages, Geol. Rev., 54, 94–104, 2008. (in Chinese with English abstract).

Tan, L., Cai, Y., Cheng, H., Edwards, L. R., Gao, Y., & Xu, H.: Centennial- to decadal-scale monsoon precipitation variations in the upper Hanjiang river region, China over the past 6650 years, Earth Planet. Sci. Lett., 482, 580–590, 2018.

Tan, L., Li, Y., Wang, X., Cai, Y., Lin, F., & Cheng, H.: Holocene monsoon change and abrupt events on the western Chinese loess plateau as revealed by accurately dated stalagmites, Geophys, Res. Lett., 47, https://doi.10.1029/2020GL090273, 2020.

Tan, M.: Circulation effect: response of precipitation $\delta^{18}O$ to the ENSO cycle in monsoon regions of China, Clim. Dynam., 42, 1067–1077, 2014.

Warken., Sophie F., Fohlmeister, J., Schröder-Ritzrau, A., Constantin, S., Spötl, C., Gerdes, A., Esper, J., Frank, N., Arps, J., Terente, M., Riechelmann, D., Mangini, A., Scholz, D.: Reconstruction of late Holocene autumn/winter precipitation variability in SW Romania from a high-resolution speleothem trace element record, Earth Planet. Sci. Lett., 499, 122–133, 2018.

Wu, Q.L, Zhao, Z.J, Liu, L., Granger, D.E, Wang, H., Cohen, D.J., Wu, X.H., Ye, M.L., Bar-Y.O., Lu, B., Zhang, J., Zhang, P.Z, Yuan, D.Y, Qi, W.Y, Cai, L.H., Bai, S.B.: Outburst flood at 1920 BCE supports historicity of China's Great Flood and the Xia dynasty, Science., 353: 579–582, 2016.

Wu, W.X., Ge, Q.S.: The possibility of occurring of the extraordinary floods on the eve of establishment of the Xia Dynasty and the historical truth of Dayu's successful regulation of floodwaters, Quarter. Sci., 25, 741–749, 2005. (in Chinese with English abstract).

Xiao, J., Si, B., Zhai, D., Itoh, S., & Lomtatidze, Z.: Hydrology of Dali lake in central-eastern Inner Mongolia and Holocene east Asian monsoon variability, J. Paleolimnology., 40, 519–528, 2008.

Xiao, J., Zhang, S., Fan, J., Wen, R., Zhai, D., & Tian, Z.: The 4.2ka event: multi-proxy records from a closed lake in the northern margin of the east Asian summer monsoon, Clim. Past., 14, 1417–1425, 2018.

Yan, M. and Liu, J.: Physical processes of cooling and mega-drought during the 4.2 ka BP event: results from TraCE-21ka simulations, Clim. Past., 15, 265–277, 2019.

Zha, X., Huang, C., Pang, J., Li, Y., Liu, J., & Cuan, Y.: Sedimentary records of Holocene palaeo-mudflow events in Tianshui basin of the western loess plateau,

https://doi.org/10.5194/cp-2021-20
Preprint. Discussion started: 15 March 2021

China, Quat. Intern., 521, 129–137, 2019.

Zhang, H., Cai, Y., Tan, L., Cheng, H., Qin, S., An, Z., Ma, L.: Large variations of $\delta^{13}C$ values in stalagmites from southeastern China during historical times: implications for anthropogenic deforestation, Boreas., 44, 511–525. 2015.

Zhang, H., Cheng, H., Cai, Y., Sptl, C., & Tan, L.: Hydroclimatic variations in southeastern china during the 4.2 ka event reflected by stalagmite records, Clim. Past., 14, 1805–1817, 2018.

Zhang, H., Griffiths, M.L., Chiang, J.C.H., Kong, W., Wu, S., Atwood, A., Huang, J., Cheng, H., Ning, Y., Xie, S.: East Asian hydroclimate modulated by the position of the westerlies during Termination I. Science., 362,580–583, 2018.

Zhang, H.W., Cheng, H., Baker, J., Kathayat, G.: Response to Comments by Daniel Gebregiorgis et al. "A Brief Commentary on the Interpretation of Chinese Speleothem $\delta^{18}O$ Records as Summer Monsoon Intensity Tracers", Quaternary., 3, 7, 2020.

Zhang, P.Z., Cheng, H., Edwards, R.L., Chen, F.H, Wang, Y.J., Yang, X.L., Liu, J., Tan, M., Wang, X.F, Liu, J.H., An, C.L., Dai, Z.B., Zhou, J., Zhang, D.Z., Jia, J.H, Jin, L.Y., Johnson, K.R.: A test of climate, sun, and culture relationships from an 1810-year Chinese cave record, Science., 322, 940–942, 2008.

Zhao, K., Wang, Y., Edwards, R.L., Cheng, H., Kong, X., Liu, D., Yang, X. L ate Holocene monsoon precipitation changes in southern China and their li nkage to Northern Hemisphere temperature, Quat. Sci. Rev., 232, https://do i.org/10.1016/j.quascirev.2020.106191, 2020.

https://doi.org/10.5194/cp-2021-20
Preprint. Discussion started: 15 March 2021

Figures and Tables

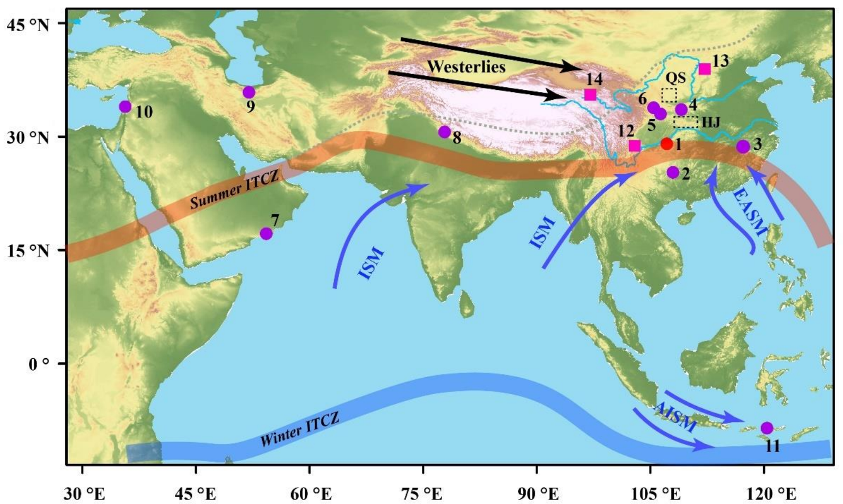

Figure 1. Location of each record. 1, Yangkou Cave (YK) (this study); 2, Dongge Cave (DG) (Wang et al., 2005); 3, Shennong Cave (SN) (Zhang et al., 2018); 4, Jiuxian Cave (Cai et al., 2010); 5, Xianglong Cave (XL) (Tan et al., 2016); 6, Wuya Cave (WY) (Tan et al., 2020); 7, Qunf Cave (Fleitmann et al., 2003); 8, Sahiya Cave (SHA)(Kathayat et al., 2017); 9, Gol-e Zard Cave (GZ) (Carolin et al., 2019); 10, Jeita Cave (Cheng et al., 2015); 11, Liang Luar Cave (LL) (Griffiths et al., 2010); 12, Yuexi Lake (YX) (Peng et al., 2021); 13, Gonghai lake (GH) (Chen et al., 2015); 14, Alake Lake (Li et al., 2021). The circles are the stalagmite records and the squares are the lake records. The two black dashed boxes represent the soil profiles in Hanjiang River Basin (HJ) and Qishui River Basin (QS), respectively. The blue arrows represent the Indian summer monsoon (ISM), the East Asian summer monsoon (EASM) and the Australian-Indian summer monsoon (AISM), respectively. The black arrows represent the

https://doi.org/10.5194/cp-2021-20
Preprint. Discussion started: 15 March 2021

Climate of the Past Discussions

westerlies. The red and blue bands of the shadow are the positions of ITCZ in summer (June-August) and winter (December-February), respectively. The dotted grey line represents the boundary of the modern summer monsoon.

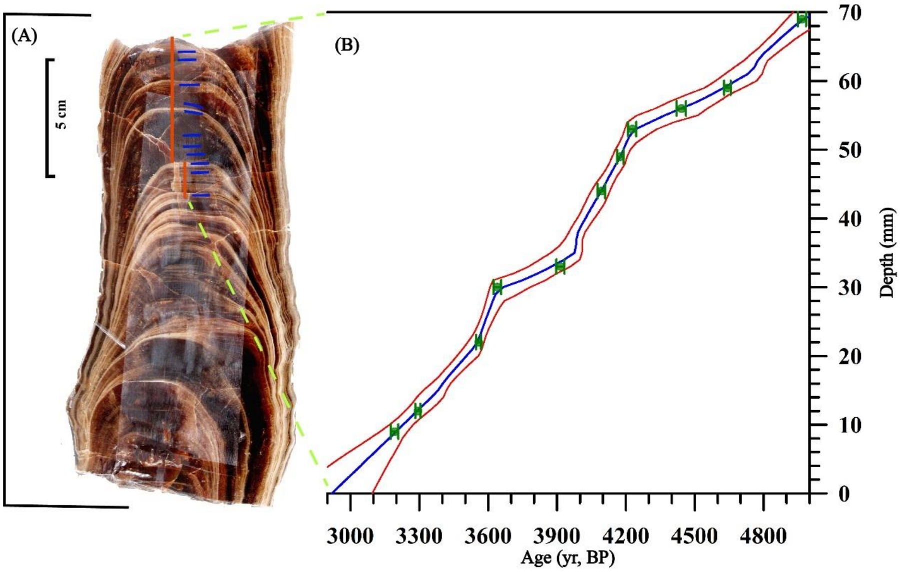

Figure 2. (A) The profile of stalagmite YK1306. The orange lines represent the sampling path of isotopes and trace elements, and the blue lines represent the sampling location of ^{230}Th dating stalagmite YK1306. (B) The chronology of stalagmite YK1306 based on Modage software (Hercman and Pawlak, 2012). The blue solid line is the chronological curve obtained using the Modage software, the red solid line represents the 95% confidence band, and the green error bar represents the dating points and the error range.

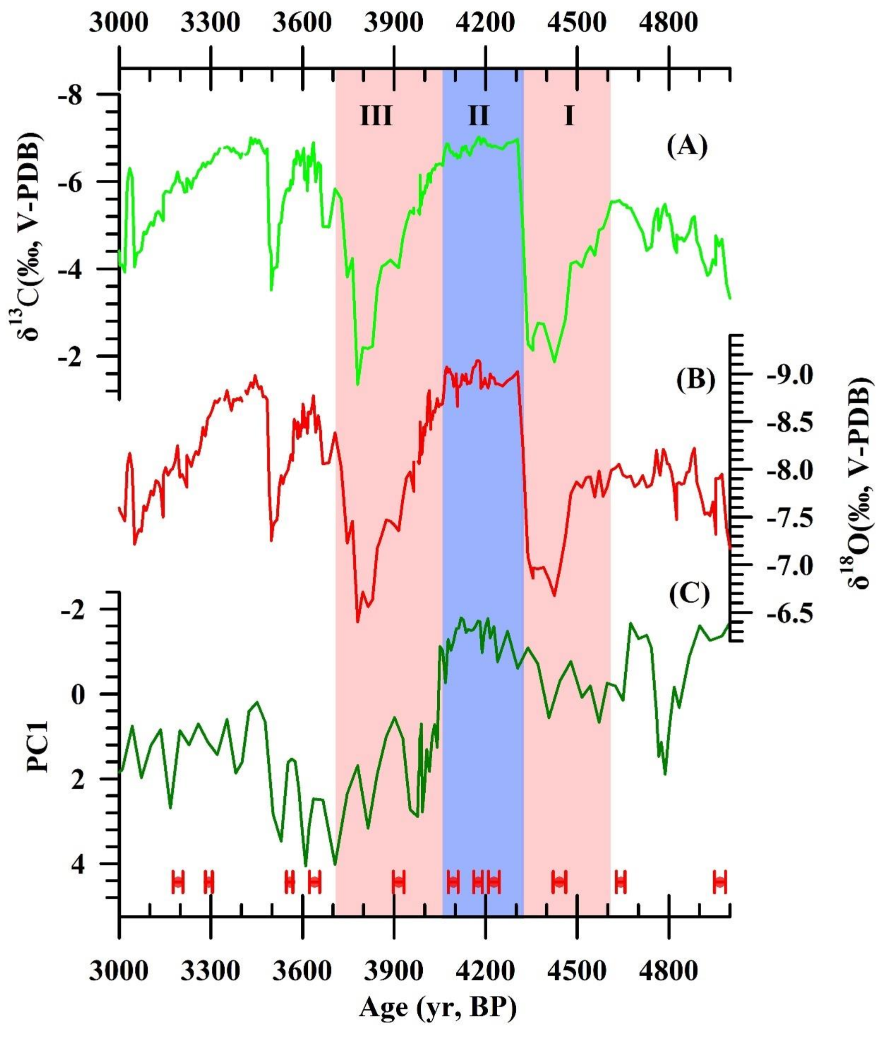

Figure 3. Comparison of multi-proxies records of stalagmite YK1306. (A) $\delta^{13}C$; (B) $\delta^{18}O$; (C) PC1 is the first principal component of Ba/Ca, Sr/Ca, Mg/Ca. The blue and pink bands represent the three stages (I–II–III) during the 4.2 ka event, respectively.

https://doi.org/10.5194/cp-2021-20
Preprint. Discussion started: 15 March 2021

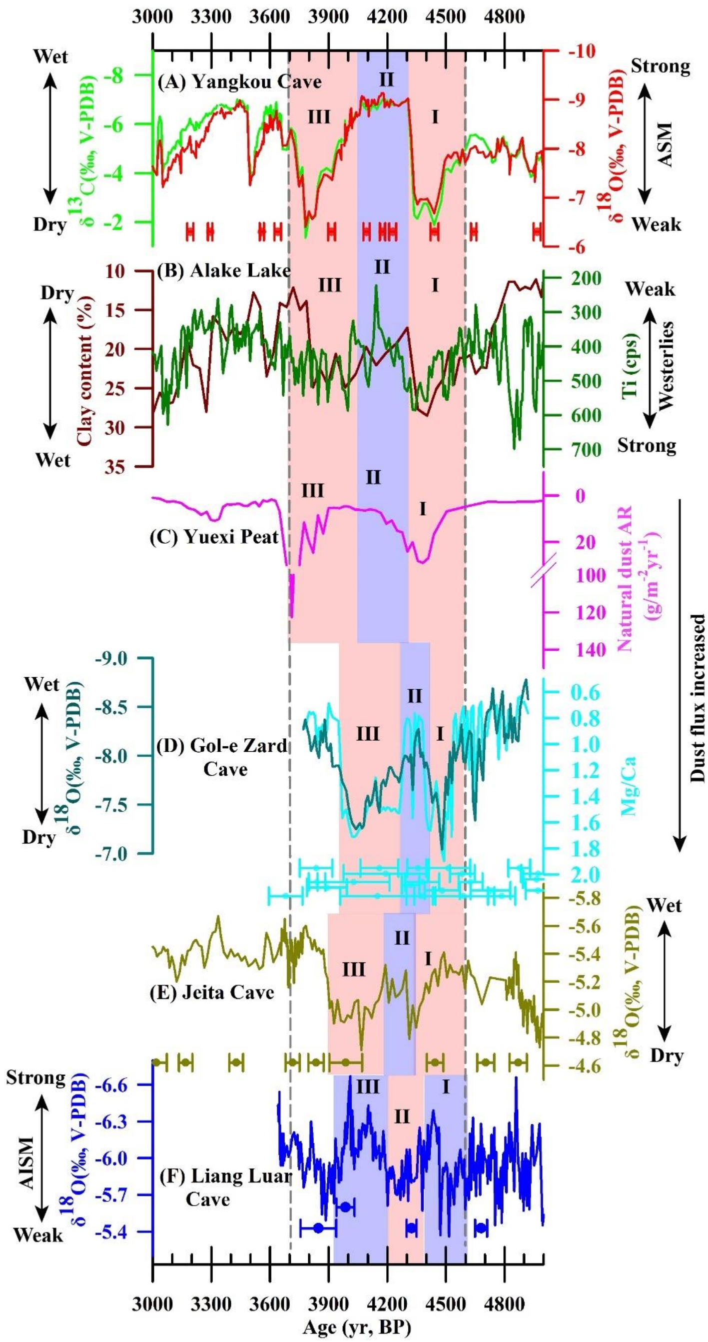

https://doi.org/10.5194/cp-2021-20
Preprint. Discussion started: 15 March 2021

Climate of the Past Discussions

Figure 4. Comparison of stalagmite records in the northern and southern Hemispheres. (A) The $\delta^{13}C$ and $\delta^{18}O$ of stalagmite YK1306 in YK Cave (this study); (B) The content of clay and Ti in Alake lake (Li et al., 2016); (C) The variations of atmospheric dust flux in YX Lake (Peng et al., 2021); (D) The Mg/Ca ratio and $\delta^{18}O$ of stalagmite in GZ Cave. The Mg/Ca indicate dust activity (Carolin et al., 2019); (E) The $\delta^{18}O$ of stalagmite in Jeita Cave (Cheng et al., 2015); (F) The $\delta^{18}O$ of stalagmite in LL Cave (Griffiths et al., 2010). The same color error bars represent its dating error. The blue and pink bands represent the three stages (I–II–III) during the 4.2 ka event, respectively.

https://doi.org/10.5194/cp-2021-20
Preprint. Discussion started: 15 March 2021

Climate of the Past Discussions

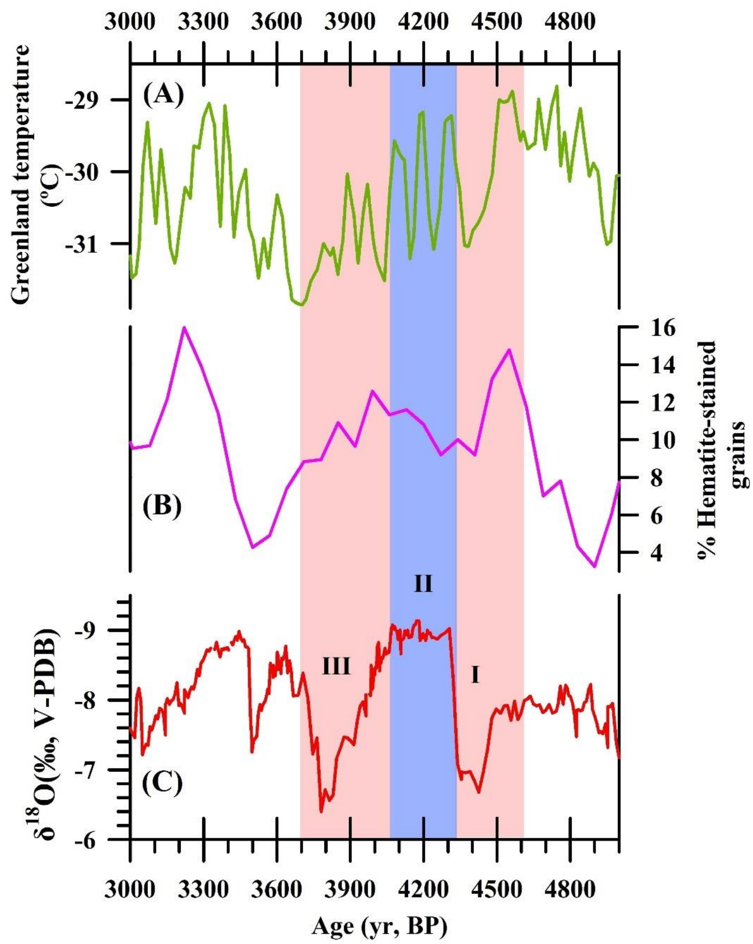

Figure 5. The driving mechanism. (A) Greenland temperature (Kobashi et al., 2017), (B) The records of drift ice (Bond et al., 2001). The blue and pink bands represent the three stages (I-II-III) during the 4.2 ka event, respectively. (C) The δ13C and δ18O of stalagmite YK1306 in YK Cave.

https://doi.org/10.5194/cp-2021-20
Preprint. Discussion started: 15 March 2021

Climate of the Past
Discussions

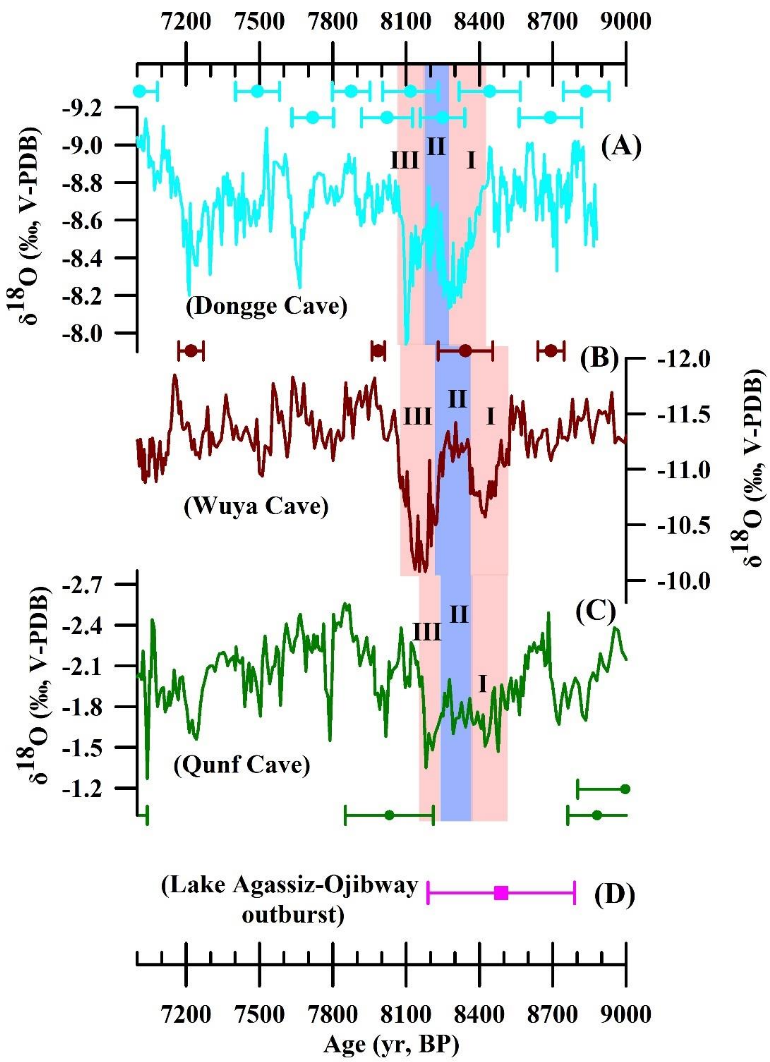

Figure 6. Comparison of stalagmite records in the ASM during the 8.2 ka event. (A) The $\delta^{18}O$ of stalagmite in DG Cave (Wang et al., 2005); (B) The $\delta^{18}O$ of stalagmite in WY Cave (Tan et al., 2020); (C) The $\delta^{18}O$ of stalagmite in Qunf Cave (Fleitmann et al., 2003). (D) Timing of Lakes Agassiz and Ojibway outburst 8470 ± 300 yr BP (Daley et al., 2011). The same color error bars represent its dating error. The blue and pink

https://doi.org/10.5194/cp-2021-20
Preprint. Discussion started: 15 March 2021

bands represent the three stages (I-II-III) during the 4.2 ka event, respectively.

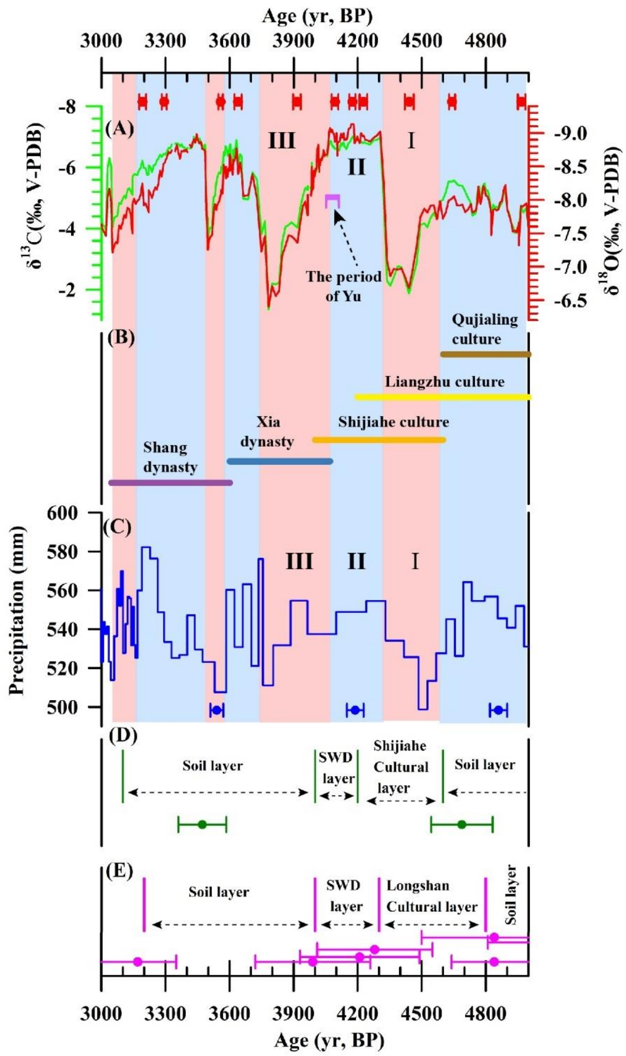

Figure 7. The comparison between the climate change and the evolution of Chinese civilization. (A) The $\delta^{13}C$ and $\delta^{18}O$ of stalagmite YK1306 in YK Cave. the purple short bar indicats the period of Yu (Yu established the Xia Dynasty); (B) Ancient civilization in the Yangtze River Valley and the Xia and Shang Dynasties; (C) Precipitation in

https://doi.org/10.5194/cp-2021-20
Preprint. Discussion started: 15 March 2021

northern China (Chen et al., 2015); (D) The soil profiles with palaeoflood slackwater deposits (SWD) in the HJ River Basin (a tributary of the Yangtze River) (Liu et al., 2015); (E) The Loess-soil profiles with SWD in QS River Basin (a tributary of the Yellow River) (Huang et al., 2011). The error bars of the same color represent its dating error. The blue bands indicate the strong ASM stage, and the pink bands indicate the weak ASM stage.

https://doi.org/10.5194/cp-2021-20
Preprint. Discussion started: 15 March 2021

Climate of the Past Discussions

Table 1. Abbreviations in this study.

Abbreviation	Full name
YK	Yangkou Cave
SN	Shennong Cave
JX	Jiuxian Cave
XL	Xianglong Cave
WY	Wuya Cave
DG	Dongge Cave
SHA	Sahiya Cave
GZ	Gol-e Zard Cave
LL	Liang Luar Cave
YX	Yuexi Lake
GH	Gonghai lake
HJ	Hanjiang River
QS	Qishui River
AOL	Lakes Agassiz and Ojibway lake
SWD	Palaeoflood Slackwater deposits
ASM	Asian summer monsoon
ISM	Indian summer monsoon
EASM	East Asian summer monsoon
AISM	Australian-Indian summer monsoon
AMOC	Atlantic Meridional Overturning Circulation
NAO	North Atlantic Oscillation
WDCR	Westerlies-dominated climatic regime
ITCZ	Intertropical Convergence Zone
PC	Principal components
PCP	Prior calcite precipitation

https://doi.org/10.5194/cp-2021-20
Preprint. Discussion started: 15 March 2021

Climate of the Past
Discussions
Open Access
EGU

Table 2 ^{230}Th dating results for stalagmite YK1306. The errors is 2σ.

Sample Number	depth (mm)	^{238}U (ppb)	^{232}Th (ppt)	^{230}Th / ^{232}Th (atomic x10^{-6})	d^{234}U* (measured)	^{230}Th / ^{238}U (activity)	^{230}Th Age (yr) (uncorrected)	^{230}Th Age (yr) (corrected)	d^{234}U$_{Initial}$** (corrected)	^{230}Th Age (yr BP)*** (corrected)
YK-1306-1	**9**	16172.0 ±25.9	243 ±24	34457 ±3417	63.9 ±1.5	0.0314 ±0.0001	3262 ±16	3261 ±16	65 ±2	**3192 ±16**
YK-1306-2	**12**	25579.1 ±42.0	740 ±26	18432 ±637	65.2 ±1.5	0.0324 ±0.0001	3363 ±11	3362 ±11	66 ±1	**3293 ±11**
YK-1306-3	**22**	2855.9 ±3.1	42 ±2	39485 ±1712	68.3 ±1.3	0.0350 ±0.0001	3627 ±10	3627 ±10	69 ±1	**3558 ±10**
YK-1306-4	**30**	15588.3 ±24.6	216 ±21	42377 ±4167	64.8 ±1.5	0.0356 ±0.0002	3709 ±17	3708 ±17	66 ±2	**3639 ±17**
YK-1306-5	**33**	13496.7 ±45.7	1452 ±30	5853 ±122	63.5 ±1.9	0.0382 ±0.0001	3988 ±17	3985 ±18	64 ±2	**3915 ±18**
YK-1306-6	**40**	15304.1 ±21.7	291 ±16	34154 ±1916	38.5 ±1.4	0.0394 ±0.0001	4211 ±13	4211 ±13	39 ±1	**4142 ±13**
YK-1306-7	**44**	18342.9 ±52.7	153 ±6	78664 ±3309	58.6 ±1.6	0.0397 ±0.0001	4164 ±16	4163 ±16	59 ±2	**4093 ±16**
YK-1306-8	**49**	1502.5 ±1.8	10 ±2	99766 ±18796	36.2 ±1.4	0.0396 ±0.0001	4244 ±14	4244 ±14	37 ±1	**4175 ±14**
YK-1306-9	**53**	14401.8 ±38.8	135 ±10	70075 ±4981	33.6 ±2.0	0.0399 ±0.0001	4297 ±18	4297 ±18	34 ±2	**4227 ±18**
YK-1306-10	**56**	9364.9 ±22.0	1397 ±31	4674 ±103	42.0 ±2.1	0.0423 ±0.0002	4516 ±20	4512 ±20	43 ±2	**4442 ±20**
YK-1306-11	**59**	15996.9 ±23.9	304 ±16	38406 ±1987	46.7 ±1.6	0.0443 ±0.0001	4712 ±14	4711 ±14	47 ±2	**4642 ±14**

U decay constants: l_{238} = 1.55125x10^{-10} (Jaffey et al., 1971) and l_{234} = 2.82206x10^{-6} (Cheng et al., 2013). Th decay constant: l_{230} = 9.1705x10^{-6} (Cheng et al., 2013).

*d^{234}U = ([^{234}U/^{238}U]$_{activity}$ – 1)x1000. ** d^{234}U$_{initial}$ was calculated based on ^{230}Th age (T), i.e., d^{234}U$_{initial}$ = d^{234}U$_{measured}$ x e^{l234xT}.

Corrected ^{230}Th ages assume the initial ^{230}Th/^{232}Th atomic ratio of 4.4 ±2.2 x10^{-6}. Those are the values for a material at secular equilibrium, with the bulk earth ^{232}Th/^{238}U value of 3.8. The errors are arbitrarily assumed to be 50%.

***B.P. stands for “Before Present” where the “Present” is defined as the year 1950 A.D.

https://doi.org/10.5194/cp-2021-20
Preprint. Discussion started: 15 March 2021

Climate of the Past Discussions

Table 3. **Principal component analysis**: eigenvalues, variance (%), and cumulative variance (%) associated to principal components.

Principal component	Eigenvalue	variance (%)	Cumulative explained variance
PC1	**2.01**	**67.15**	**67.15**
PC2	0.84	28.14	95.29
PC3	0.14	4.71	100